




Enhancement of the magnetoelectric effect in the $\text{Bi}_2\text{Fe}_4\text{O}_9/\text{BiFeO}_3$ composite as a result of dipole and migration polarization in mullite

L. V. Udod^{1,2,*} , S. S. Aplesnin^{1,2}, F. V. Zelenov², M. N. Sitnikov², M. S. Molokev¹, and O. B. Romanova¹

¹ Federal Research Center KSC SB RAS, Kirensky Institute of Physics, Akademgorodok 50, bld. 38, Krasnoyarsk, Russia 660036

² Reshetnev Siberian State University of Science and Technology, Krasnoyarsk, Russia 660037

Received: 15 February 2024

Accepted: 7 June 2024

Published online:
14 June 2024

© The Author(s), under exclusive licence to Springer Science+Business Media, LLC, part of Springer Nature, 2024

ABSTRACT

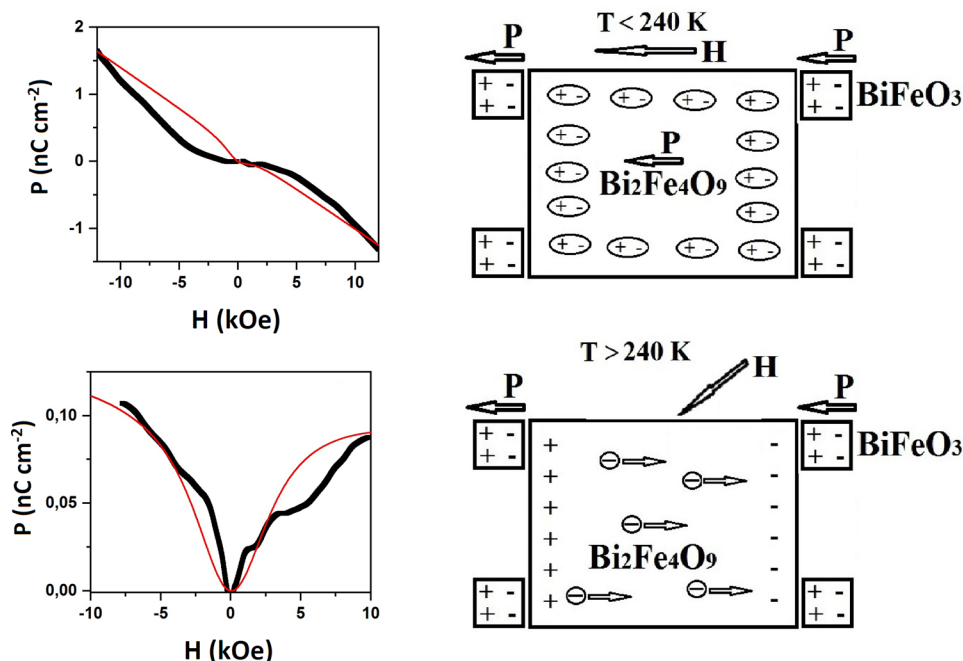
The effect of the size of $\text{Bi}_2\text{Fe}_4\text{O}_9$ and BiFeO_3 nanoparticles on the magnetoelectric interaction in the $\text{Bi}_2\text{Fe}_4\text{O}_9/\text{BiFeO}_3$ composite with a percentage ratio of 67/33 has been studied. The electrostriction and electric polarization on electric and magnetic field in wide temperature range has been measured. The hysteresis of the polarization and I – V characteristics has been found. Temperature ranges with activation and hopping types of conductivity have been found. The mechanism of electric polarization and the crossover temperature from dipole polarization to migration polarization at 260 K have been established. Linear and quadratic contributions to the magnetoelectric effect have been found. Below 120 K the linear contribution is an order of magnitude greater than the quadratic contribution and above 240 K the quadratic contribution to the ME effect prevails. Models have been proposed to explain the enhancement of the magnetoelectric effect as a result of the migration polarization in mullite and linear magnetoelectric effect in bismuth ferrite. The correlation of temperatures of the extremum of the temperature coefficient of the electrical resistance and the magnetic phase transition in mullite at 260 K indicates a polaron-type conductivity and a strong electron–phonon interaction. A change in the sign of the electrostriction coefficient upon heating and the compression temperature of the composite in an electric field was found.

Handling Editor: David Cann.

Address correspondence to E-mail: luba@iph.krasn.ru

<https://doi.org/10.1007/s10853-024-09885-x>

GRAPHICAL ABSTRACT



Introduction

Interest in multiferroics is due to the discovery of gigantic values of the magnetoelectric (ME) effect in them [1], which can be used in advanced electronic devices, including memory cells, touch sensors, solar cells, etc. [2–4]. Multiferroics used as magnetic field sensors can become an alternative to Hall sensors and colossal magnetoresistance materials. The advantage of multiferroic sensors is the absence of Joule heat at the electric current flow through a sample.

Bismuth ferrite BiFeO₃ (BFO) is a compound with the ME interactions, which exhibits simultaneously the ferroelectric and (anti)ferromagnetic properties at room and higher temperatures (its Curie temperature is $T_C = 1083$ K and Néel temperature is $T_N = 673$ K) [1]. Due to this fact, BFO is a candidate for creation of new generation electronic devices in which the magnetic properties are controlled by a low-energy electric field [5–7].

Ferroelectricity in BFO is known to be related to the stoichiometric activity of the Bi³⁺ ion [8]. The polarization value in BFO depends on the synthesis conditions: in particular, at room temperature, the polarization of its thin films is 50–90 $\mu\text{C}/\text{cm}^2$ [1]. The polarization of ceramic samples is 8.9 $\mu\text{C}/\text{cm}^2$ [9, 10];

in single crystals, it amounts to 61 $\mu\text{C}/\text{cm}^2$ at 77 K [11] with an unsaturated hysteresis loop and can attain $P_s \sim 100$ $\mu\text{C}/\text{cm}^2$ along the [111] crystallographic axis [12, 13]. The electric polarization is maintained in nanoparticles 45–70 nm in size on an Au/Ti/SiO₂/Si substrate [14] and 25-nm nanoparticles exhibit the butterfly-shaped piezoelectric hysteresis [14]. In the BFO thin films with a grain size of 1–2 μm , the residual polarization increases sharply above $T = 165$ K [15, 16].

Bismuth ferrite is a multifunctional oxide with a distorted rhombohedral perovskite structure (sp. gr. $R3c$) [17]. The adjacent Fe³⁺ ions are coupled by the Dzyaloshinskii–Moriya interaction, which leads to an antiferromagnetic spin cycloid [17] with a wavelength of 62 nm [18] and the ME interactions in bulk samples at 4 K [16, 19]. Strengthening of the ME effect is achieved when the nanoparticle size decreases below the spin cycloid period [17–20].

ME effect is found in composite compounds based on BiFeO₃. For example, the influence of sol–gel synthesis method technology of the BiFeO₃–BaFe₁₂O₁₉ composite compound on magnetic properties was studied. It has been established that as the particle size decreases, the magnetoelectric interaction and magnetic energy increase [21]. Composite (1-x) BaFe₁₂O₁₉–(x)BiFeO₃; (x = 0.05, 0.08 and 0.10), obtained

by standard solid-phase reaction, exhibits multiferroic properties [22]. A mild anomaly in dielectric constant and $\tan\delta$ near Neel temperature of BiFeO_3 evidences ME effect in composites. An increase of the ME coefficient is observed.

Composite system $0.8\text{BiSm}_x\text{Fe}_{1-x}\text{O}_3-0.2\text{PbTiO}_3$ with ($x = 0:05, 0.10, 0.15, \text{ and } 0.20$) was prepared by using the conventional solid-state reaction method [23]. The remnant polarization decreases with the increase of Sm concentration. An increase in resistivity has been observed with increase in Sm concentration as the values of the dielectric constant and loss tangent decrease. The AC conductivity obtained from the dielectric data exhibits Arrhenius-type electrical conductivity and the value of activation energy increases with increase in x .

Mullite $\text{Bi}_2\text{Fe}_4\text{O}_9$, with an orthorhombic crystal structure (sp. gr. *Pbam*) exhibits the weak ferroelectric properties [24, 25]. In the vicinity of the magnetic ordering temperature, the resistivity increases by two orders of magnitude and the electric polarization hysteresis appears [26]. The shift of the anomaly of the dielectric losses toward higher temperatures in a magnetic field proves the existence of the ME interaction in mullite [26].

The magnetic and ferroelectric properties of the polycrystalline $\text{Bi}_2\text{Fe}_4\text{O}_9$ compound depend strongly on the grain size and synthesis technique used. The samples with a grain size of 60 nm have a canted antiferromagnetic structure with the minor magnetization. As the grain size increases the Néel temperature shifts toward higher temperatures. A ferroelectric hysteresis loop is observed at room temperature for the samples with a grain size larger than 200 nm. The residual polarization increases with the grain size. Mullite with a grain size of 900 nm has a high residual polarization ($0.21 \mu\text{C cm}^{-2}$) [27]. The room-temperature residual polarization of single-crystalline nanotubes is $0.02 \mu\text{C cm}^{-2}$ [28]. The nanosized $\text{Bi}_2\text{Fe}_4\text{O}_9$ compound with a grain size of 5 nm synthesized by the sonochemical technique exhibits the polarization hysteresis. As the grain size increases to 50 nm, the width of the hysteresis loop in an external electric field up to 7 kV cm^{-1} increases, the residual polarization amounts to $P_r = 0.29 \mu\text{C cm}^{-2}$, and the coercivity is $E_c = 12.39 \text{ kV cm}^{-1}$ [29].

The ME properties of the $\text{Bi}_2\text{Fe}_4\text{O}_9$ compound can be improved by creating composite materials, for example, $\text{CoFe}_2\text{O}_4/\text{Bi}_2\text{Fe}_4\text{O}_9$. The CoFe_2O_4 compound exhibits the magnetostrictive properties and induces

the lattice strain and electric polarization in the composite [30].

The BiFeO_3 compound is characterized by the G-type antiferromagnetic ordering, at which a spatially modulated structure (SMS) with a period of $\lambda = 620 \pm 20 \text{ \AA}$ is formed. The destruction of the SMS by an external magnetic field or replacement of bismuth ions by rare-earth and $3d$ ions causes ferromagnetism and the ME interaction [31–34]. The SMS in the composites becomes energetically unfavorable. In particular, the nanocomposites based on perovskite-like bismuth orthoferrite BiFeO_3 and mullite-like ferrite $\text{Bi}_2\text{Fe}_4\text{O}_9$ demonstrate the effects related to the exchange interactions at the interface between these phases [35, 36]. The BiFeO_3 (90–94%)– $\text{Bi}_2\text{Fe}_4\text{O}_9$ (10–6%) nanocomposites exhibit an anomalous exchange bias (300–600 Oe) upon cooling in zero magnetic field. This behavior is explained by the interaction between ferromagnetic $\text{Bi}_2\text{Fe}_4\text{O}_9$ with a grain size of 13–19 nm and BiFeO_3 with a canted antiferromagnetic structure and a grain size of 57–112 nm [35].

Particular interest to bismuth ferrite is due to the fact that it demonstrates a strong correlation of structural, electrical, and magnetic properties, high temperatures magnetic and electrical orders, poor conductivity [37], and gigantic values of ME and MDE effects [38]. All this allows this material to be used for practical use over a wide temperature range and in relatively small fields.

We synthesized the $\text{Bi}_2\text{Fe}_4\text{O}_9/\text{BiFeO}_3$ composite consisting of the $\text{Bi}_2\text{Fe}_4\text{O}_9$ (67%) and BiFeO_3 (33%) components with a $\text{Bi}_2\text{Fe}_4\text{O}_9$ grain size of 1.5–4.0 μm . The BiFeO_3 grain size is less than the resolution of a scanning electron microscope (100 nm) [39]. The feature of this percentage ratio is related to the high magnetostriction. The composites with such a percentage ratio of the phases and grain sizes have not been synthesized so far.

The $\text{Bi}_2\text{Fe}_4\text{O}_9/\text{BiFeO}_3$ (67/33%) composite should have the multiferroic properties. The electrical resistance of mullite decreases sharply above the magnetic ordering temperature and charge transfer is accompanied by the local lattice strain. An external electric field induces the electric polarization in mullite, which leads to the deformation of the sample as a result of the electronic compressibility. In an external magnetic field, an electric field is induced in bismuth ferrite nanoparticles surrounding mullite grains under the ME interaction, which should enhance the ME effect and electrostriction.

At present, there is no information in the literature about the magnetoelectric effect in the $\text{Bi}_2\text{Fe}_4\text{O}_9/\text{BiFeO}_3$ composite system. The aim of this work is to study magnetoelectric interaction and electrostriction of $\text{Bi}_2\text{Fe}_4\text{O}_9/\text{BiFeO}_3$ (67/33%) composite.

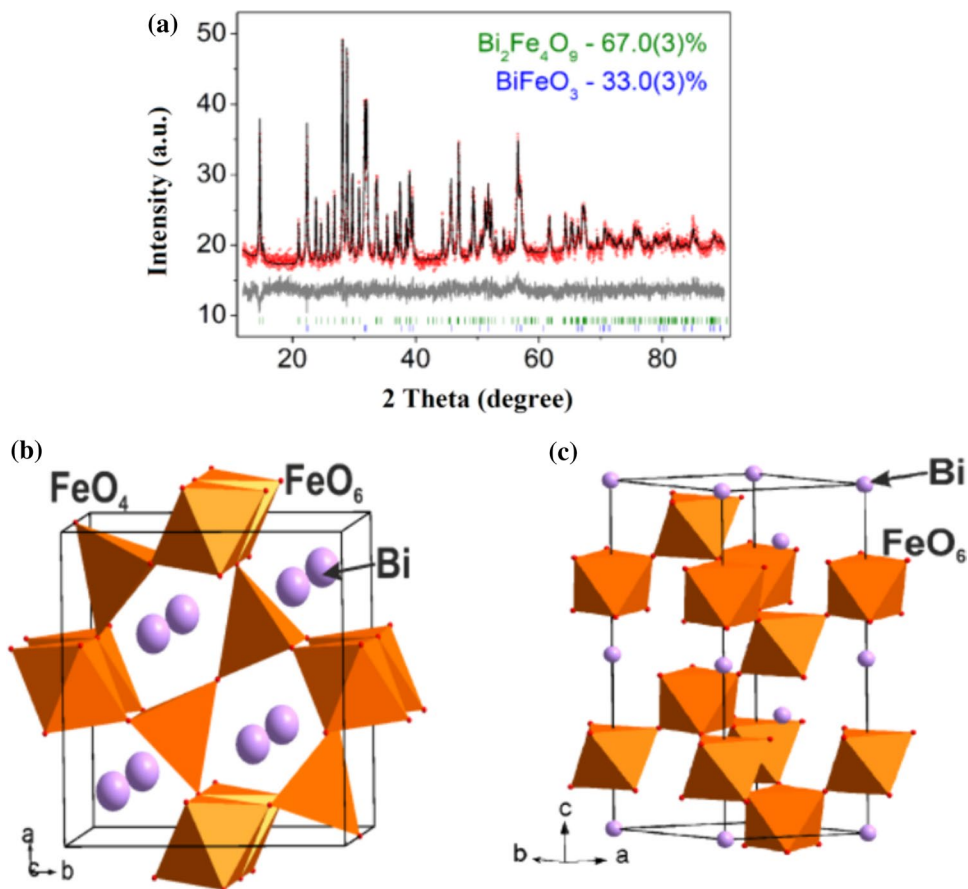
These studies fill the gap in the mechanism of ME interactions in composites containing single-domain ferroelectric particles and semiconductor granules with migratory polarization.

Material and methods

The $\text{Bi}_2\text{Fe}_4\text{O}_9/\text{BiFeO}_3$ composite was synthesized by the solid-phase reaction using the technique described in [39]. The powder diffraction data on the composite for the Rietveld refinement were collected at room temperature on a Bruker D8 ADVANCE powder diffractometer (Cu- $K\alpha$ radiation) with a VANTEC linear detector at the Krasnoyarsk Regional Center for Collective Use of the Krasnoyarsk Scientific Center, Siberian Branch of the Russian Academy

of Sciences. The 2θ angle step was 0.016° and the counting time was 2 s per step. These structures [40, 41] were taken as a starting model for the Rietveld refinement, which was performed using the TOPAS 4.2 software [42]. Atomic coordinates were fixed due to mixing of the compounds and overlap of the main peaks. Overlapping peaks from different phases can result in strong correlations between refined parameters, leading to a decrease in the overall reliability of all refined parameters. The refinement was stable and yielded the low R factors ($R_{wp} = 5,93\%$, $R_p = 4,65\%$, $\chi^2 = 1,23$). According to the X-ray diffraction data, the $\text{Bi}_2\text{Fe}_4\text{O}_9/\text{BiFeO}_3$ composite consists of $\text{Bi}_2\text{Fe}_4\text{O}_9$ (67%) and BiFeO_3 (33%), and difference Rietveld plot (Fig. 1a) shows the absence of extra peaks which can be associated with additional impurity phases. Figure 1b and c shows the $\text{Bi}_2\text{Fe}_4\text{O}_9$ and BiFeO_3 structures obtained by X-ray diffraction analysis. The $\text{Bi}_2\text{Fe}_4\text{O}_9$ compound has an orthorhombic crystal structure (sp. gr. *Pbam*) (Fig. 1b), which is consistent with the data reported in [43]. The first iron ion is coordinated by four oxygen ions with

Figure 1 **a** XRD pattern of the $\text{Bi}_2\text{Fe}_4\text{O}_9/\text{BiFeO}_3$ composite. The upper curve shows the experimental XRD pattern; the middle curve, the theoretical XRD pattern; and the lower curve, the difference between the theoretical and experimental XRD patterns. **b** Crystal structure of $\text{Bi}_2\text{Fe}_4\text{O}_9$. **c** Crystal structure of BiFeO_3 .



the formation of FeO_4 tetrahedra, while the second iron ion is coordinated by eight oxygen ions with the formation of FeO_6 octahedra. These polyhedra are interconnected through nodes, creating a 3D net structure. Bismuth ferrite BiFeO_3 has a rhombohedral structure (sp. gr. $R3c$). The asymmetric part of the BiFeO_3 unit cell comprises one iron ion, one bismuth ion, and one oxygen ion (Fig. 1c). Each iron ion is coordinated by six oxygen ions with the formation of FeO_6 octahedra. These octahedra are interconnected through nodes and create a 3D net. In addition, bismuth ions are positioned within voids in the structure.

Changes in the linear sizes of the sample (dL/L) in an electric field were measured with strain gauges. The sample with a strain gauge attached was placed in an external electric field. The sample deformation coefficient was calculated using the formula

$$\beta = (R(E) - R(E = 0))/R(E = 0),$$

where $R(E)$ and $R(E = 0)$ are the strain gauge resistances measured in an external electric field and without it.

The electric polarization was measured on pellet-shaped samples using a Keithley 6517B electrometer. The ME interaction was established from the induced electric polarization in magnetic fields of up to 13 kOe. The dc study of the electrical properties was carried out by a two-probe method using a 344 10A Agilent Technologies multimeter in the temperature range of 80–400 K.

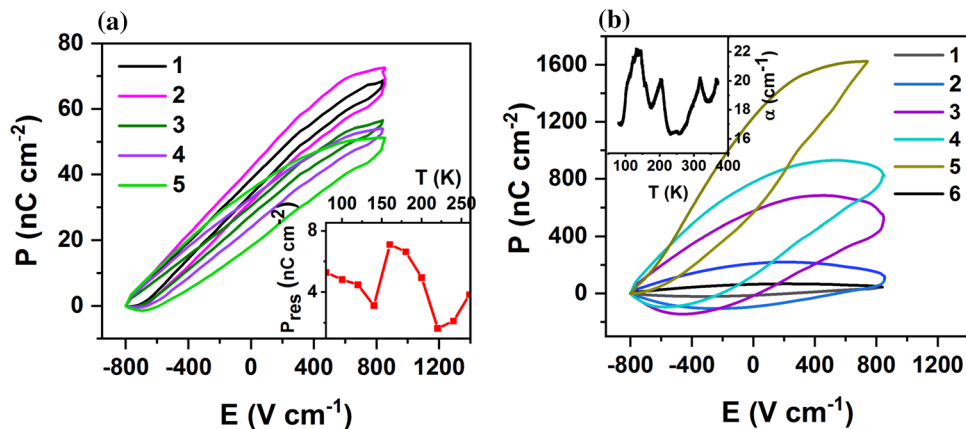


Figure 2 The polarization of $\text{Bi}_2\text{Fe}_4\text{O}_9/\text{BiFeO}_3$ composite versus external electrical field at different temperatures **a** Curve 1 corresponds to temperature $T = 80$ K, 2–180, 3–240, 4–280, 5–300 K. The inset shows the temperature dependence of residual polariza-

Results and discussion

Analysis of polarization

The field dependence of the electric polarization of the $\text{Bi}_2\text{Fe}_4\text{O}_9/\text{BiFeO}_3$ composite at different temperatures presented in Fig. 2 is characterized by a hysteresis loop and residual polarization (inset in Fig. 2a) with two minima at $T = 140$ and 220 K. The first minimum is related to the surface structural transition in BiFeO_3 without changes in the crystal structure symmetry at 140 K, which is accompanied by a sharp change in the sample volume and anomalies in the impedance spectrum in bismuth ferrite nanotubes [44]. For the $\text{Bi}_2\text{Fe}_4\text{O}_9/\text{BiFeO}_3$ composite, anomalies in the temperature dependence of the sound damping coefficient (inset to Fig. 2b), thermal expansion coefficient, and magnetostriction were found at this temperature [39]. The thermal expansion coefficient maximum at 150 K in zero magnetic field shifts to a temperature of 163 K in a magnetic field of $H = 12$ kOe. The temperatures of the maximum magnetostriction constant and the ultrasound damping coefficient are corresponds with a temperature of $T = 140$ K of the structural surface phase transition in BiFeO_3 . The BiFeO_3 lattice constant increases sharply above 140 K [44], which is in qualitative agreement with our data.

The next $P_S(T)$ minimum at $T = 220$ K is attributed to the disappearance of magnetic order in mullite ($T = 240$ K) [45]. At low temperatures, the spontaneous polarization of the $\text{Bi}_2\text{Fe}_4\text{O}_9/\text{BiFeO}_3$ composite is

zation. **b** Curve 1 corresponds to temperature $T = 320$ K, 2–340, 3–360, 4–380, 5–390 K. The inset of figure **b** shows the temperature dependence of sound damping coefficient of $\text{Bi}_2\text{Fe}_4\text{O}_9/\text{BiFeO}_3$ composite.

dipole-type, which is mainly caused by BiFeO_3 nanoparticles. The polarization in mullite $\text{Bi}_2\text{Fe}_4\text{O}_9$ below the Néel temperature is caused by a lone electron pair on the bismuth ion, the asymmetric arrangement of the nearest oxygen ions [46]. With an increase in temperature from $T = 240$ K, the migration polarization is induced. It occurs due to the diffusion of electrons over anionic vacancies. Under the action of an external electric field, electrons are redistributed among vacancies and the localization of electrons causes a local increase in the volume of the impurity state, which leads to the broadening of the electric polarization hysteresis loop.

Thus, above 240 K, the magnetic order in mullite vanishes and the migration contribution of mullite to the polarization occurs. It significantly exceeds the dipole contribution to the polarization from bismuth ferrite BiFeO_3 confirmed by the analysis of the I – V characteristics.

Analysis of I – V characteristics

The I – V characteristics of the $\text{Bi}_2\text{Fe}_4\text{O}_9/\text{BiFeO}_3$ composite are nonlinear over the entire temperature range under study (Fig. 3) and reveal hysteretic. Up to $T = 200$ K, the hysteresis is symmetric; above this temperature, the asymmetry of the hysteresis loops is observed (inset to Fig. 3b). A current in zero electric field is the polarization current $I = (dP/dt)(dt/dU)$. Above 240 K, the I – V characteristic of the $\text{Bi}_2\text{Fe}_4\text{O}_9/\text{BiFeO}_3$ composites exhibits the memristor properties with the bistable current states and the asymmetry of the I – V characteristic appears. The hysteresis acquires the butterfly shape (Fig. 3b). An internal electric field is induced in the sample by the migration polarization of mullite.

The hysteresis of the I – V characteristic is caused by the Coulomb attraction of electrons and holes on the surface of mullite grains with the dipole moments of bismuth ferrite. Under the action of an external field, charges are induced on the surface of mullite particles, which screen the electric polarization of bismuth ferrite nanoparticles. The Coulomb interaction between the surface charges of mullite and bismuth ferrite particles determines the coercivity necessary for reorientation of the electric polarization (Fig. 2). When measuring the current–voltage characteristic, the external electric field changes the direction of the electric polarization vector of bismuth ferrite granules. As a result, an internal electric field is induced in the composite. BiFeO_3 particles have a coercive field. To reorient the dipole moment, it is necessary to apply an external electric field exceeding the coercive field of bismuth ferrite. Therefore, the hysteresis of the current–voltage characteristic and polarization correlate with each other.

Analysis of electrical resistance

The temperature dependence of the electrical resistance of the $\text{Bi}_2\text{Fe}_4\text{O}_9/\text{BiFeO}_3$ composite is shown in Fig. 4. In the low-temperature region, the resistance depends weakly on temperature and decreases by five orders of magnitude upon heating. The resistivity of the $\text{Bi}_2\text{Fe}_4\text{O}_9/\text{BiFeO}_3$ composite at $T = 300$ K is $\rho = 2.7 \cdot 10^8 \Omega \text{ cm}$ and, for pure BiFeO_3 , $\rho \sim 6 \cdot 10^{10} \Omega \text{ cm}$ [47]. At $T = 340$ K, the conductivity in the composite changes from activation-type with an activation energy of $\Delta E = 0.67$ eV to hoppings with variable length. Hopping conductivity with hoppings variable length is a model used to describe the transport of charge carriers in a disordered conductor by hopping over a wide

Figure 3 The I – V characteristics of $\text{Bi}_2\text{Fe}_4\text{O}_9/\text{BiFeO}_3$ composite at different temperatures. **a** Curve 1 corresponds to temperature $T = 80$ K, 2–160, 3–200 K. **b** Curve 1 corresponds to temperature $T = 280$ K, 2–320, 3–360 K. The inset of figure **b** shows the I – V characteristics at temperature $T = 280$ K.

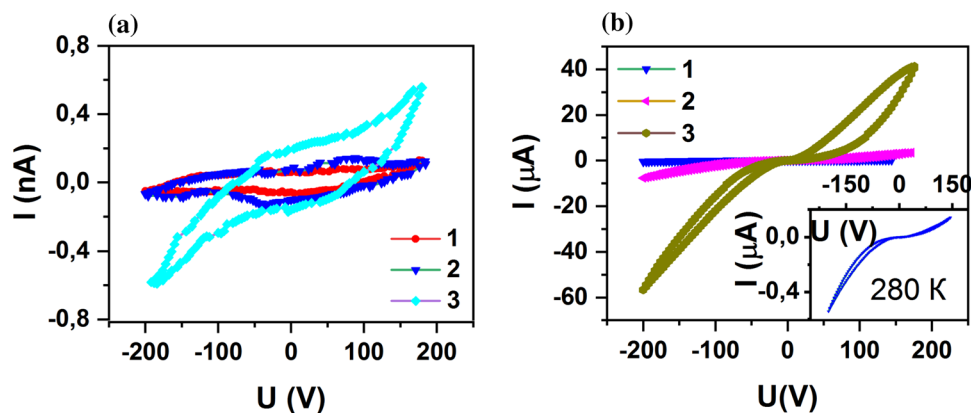
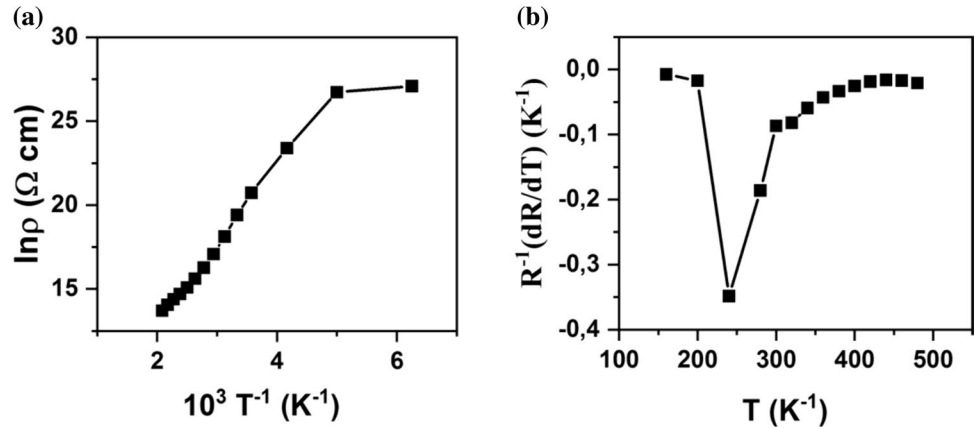


Figure 4 **a** The temperature dependence of the electrical resistance of the Bi₂Fe₄O₉/BiFeO₃ composite. **b** The temperature coefficient of the electrical resistance (dR/dT) R^{-1} of the Bi₂Fe₄O₉/BiFeO₃.



temperature range [48]. Electron jumps occur from one impurity to another without the participation of a zone of delocalized states. If electronic states are localized near the Fermi level, then an electron located below the Fermi level jumps to a state slightly above it. In this case, the hopping length is compared with the damping length of the hydrogen-like localized wave function of the electron. The temperature dependence of hopping conductivity is determined by the shape of the density of electronic impurity states at the Fermi level. The crossover temperature from one conductivity mechanism to another depends on the impurity concentration.

With a further decrease in temperature to 240 K, electrons are localized in potential wells with the tunnel conductivity.

At the temperature of the magnetic phase transition in mullite ($T = 240$ K), the temperature coefficient of the electrical resistance $(dR/dT)R^{-1}$ has an extremum (Fig. 4b), which indicates a polaron-type conductivity and a strong electron–phonon interaction.

Analysis of magnetoelectric effect

In frustrated spin systems, the transition to an ordered magnetic state causes crystal structure distortions with a breach of the inversion center, which leads to the ME interaction. This mechanism of the onset of the ME effect was observed in the YMnO₃, TbMnO₃, and HoMnO₃ compounds [49, 50]. In addition, the ME effect can be caused by a lone electron pair of bismuth ions or displacement of oxygen ions in a magnetic field due to the spin–orbit and exchange striction interactions.

The Bi₂Fe₄O₉ compound is an antiferromagnet with a noncollinear magnetic structure and frustrated exchange interactions [51]. The ME interaction in the Bi₂Fe₄O₉/BiFeO₃ composite was established from the magnetic field-induced electric polarization. Figure 5 shows the field dependence of the induced polarization in magnetic fields at temperature of 80, 120, 200, 240, 300, 320, and 360 K.

The polarization induced by a magnetic field is fitted by the two terms:

$$P = aH + b \frac{H^2}{1 + dH^2}, \tag{1}$$

where a , b , and d are the fitting parameters. The function (1) is satisfactory describe the experimental data (Fig. 5). The linear ME effect is caused by the displacement of Bi³⁺ and Fe³⁺ ions along the [111] direction of the pseudocubic perovskite unit cell of BiFeO₃ granules, which is confirmed experimentally and theoretically [52]. The quadratic effect is associated with migration polarization in Bi₂Fe₄O₉ granules. Electron diffusion in mullite occurs under the electric field induced by BiFeO₃ particles in a magnetic field.

The electron diffusion in mullite occurs under the influence of an electric field induced by BiFeO₃ particles in a magnetic field. As a result, a potential difference $\Delta\varphi \sim P/r^2$ arises in Bi₂Fe₄O₉, where P —polarization, r —distance. In a magnetic field, the induced electric polarization (P) in the direction of the field decreases. Polarization is proportional to current density $P \sim j$. Let us represent the change in polarization in the form $\Delta P = P(H) - P(0) \sim (j(H) - j(0))$. Current density in the field is $j(H) = \frac{\sigma E}{1 + (\omega_c \tau)^2}$ and in zero magnetic field.

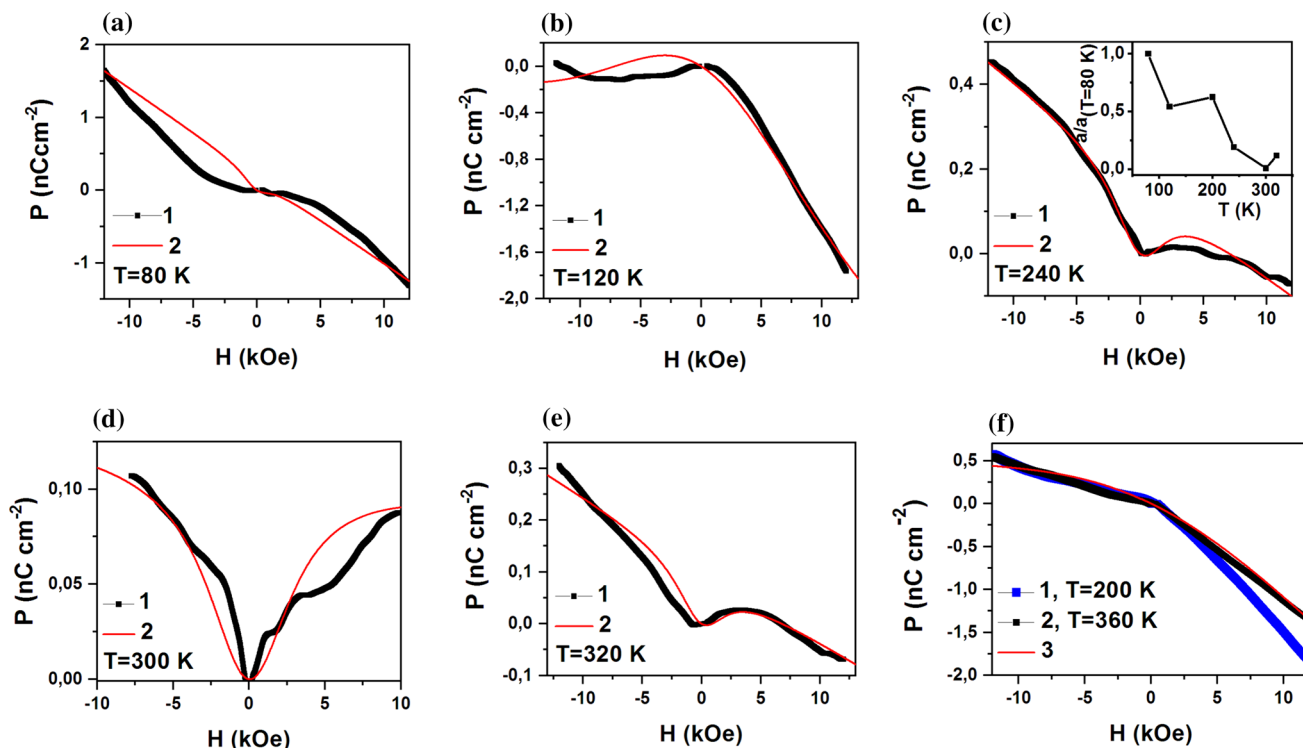


Figure 5 The polarization of $\text{Bi}_2\text{Fe}_4\text{O}_9/\text{BiFeO}_3$ versus magnetic field at different temperatures. **a–e** Curve 1 corresponds to experimental data, curve 2 corresponds to fitting function according to (1). **f** Curves 1 and 2 corresponds to experimental data, curve

3 corresponds to fitting function according to (1). The inset of figure **c** shows the temperature dependence of the relative linear coefficient of ME ($a/a(T=80\text{ K})$).

$j(0) = \sigma E; \Delta j = j(H) - j(0) \Rightarrow \Delta j = -\frac{(\omega_c \tau)^2}{1 + (\omega_c \tau)^2}$, where ω_c is the cyclotron frequency for a free electron $\omega_c = eB/m$ (e —electron charge and m —electron mass, B —magnetic field induction), τ —relaxation time in a magnetic field, which obeys the Arrhenius law.

$\tau = \tau_0 \exp(\Delta E/kT)$. Hence the change in induced electric polarization in a magnetic field has the form [53]:

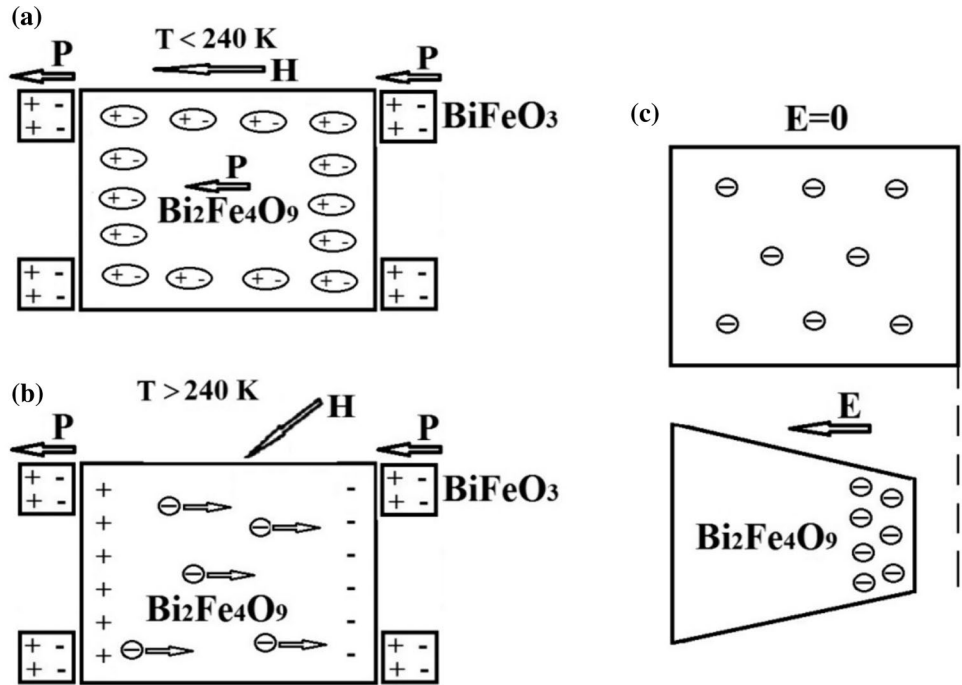
$$\Delta P = \int \Delta j dt \sim \frac{(\omega_c \tau)^2}{1 + (\omega_c \tau)^2}$$

Below 120 K the linear contribution is an order of magnitude greater than the quadratic contribution. In the temperature range 120 K–240 K, the linear and quadratic contribution differs slightly in magnitude, and above 240 K the quadratic contribution to the ME effect prevails. It is possible that ferrons exist in this temperature range, i.e., the spins of conduction electrons polarize localized spins, and an external magnetic field can change the mobility of ferrons or spin polarons. This is qualitatively confirmed by

the magnetic susceptibility of the $\text{Bi}_2\text{Fe}_4\text{O}_9/\text{BiFeO}_3$ composite with a broad maximum in the range of the magnetic phase transition of $\text{Bi}_2\text{Fe}_4\text{O}_9$ from the antiferromagnetic to paramagnetic state [39]. At $T > 320\text{ K}$, conductivity and mobility in mullite increase and a Hall potential difference is induced in mullite grains, which is proportional to the square of the magnetic field strength. The electric current in mullite is created by the electric field of BiFeO_3 particles as a result of the linear magnetoelectric effect. The linear coefficient of ME interaction has a negative sign ($a < 0$) and $a = -1,5 \cdot 10^{-13}\text{ C}/(\text{cm}^2\text{ kOe})$ at $T = 80\text{ K}$. The temperature dependence of the linear coefficient of ME interaction is presented in the inset to Fig. 5c. A negative linear magnetoelectric coupling was observed in BiFeO_3 [54].

This effect can be explained within the core–shell model. An external magnetic field and the linear ME effect induce an electric field in bismuth ferrite nanoparticles, which leads to the electric polarization of mullite at $T < 240\text{ K}$ (Fig. 6a). As a result, the overall polarization of the composite increases. At heating $T > 240\text{ K}$ the electric field in bismuth ferrite cause the

Figure 6 **a** Dipole polarization of the $\text{Bi}_2\text{Fe}_4\text{O}_9/\text{BiFeO}_3$ composite induced by the external magnetic field. **b** The linear ME effect under magnetic field induces an electric field in bismuth ferrite nanoparticles, which leads to the migration polarization of mullite grains. **c** The compression of the $\text{Bi}_2\text{Fe}_4\text{O}_9$ grain under electric field above room temperature as a result of the electron compressibility.



migration polarization of mullite grains (Fig. 6b). A change in the magnetic field polarity causes a change in the electric field sign and, consequently, leads to a change in the mullite polarization sign.

Analysis of electrostriction

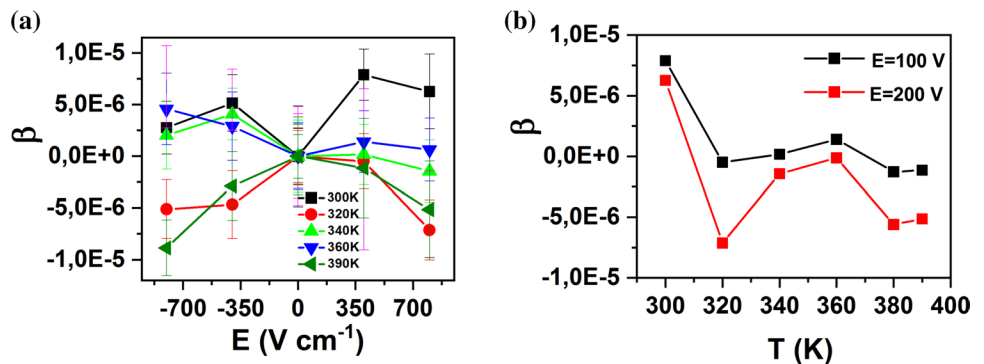
Electrostriction is the deformation of semiconductor materials in an electric field, which is proportional to the squared electric field strength: $\Delta R/R = \beta E^2$ [55], where β is the electrostriction coefficient depending on the compressibility, density, and permittivity. Delocalization of electrons and their redistribution over a sample cause deformation of a sample in the applied

electric field direction. The electrostriction effect is even (quadratic).

Figure 7 shows the electric field dependence of the linear sizes of the $\text{Bi}_2\text{Fe}_4\text{O}_9/\text{BiFeO}_3$ sample. The dependence of the striction coefficient from the electric field can be qualitatively described by the linear and quadratic contribution $\beta = aE + bE^2$, where a and b are the fitting parameters. At all temperatures, the quadratic dependence associated with the electrostriction of mullite predominates. The piezoelectric contribution is due to bismuth ferrite particles. Therefore, the striction coefficient does not coincide at the polarity of the electric field changes (Fig. 7a).

Figure 7b presents the temperature dependence of the electrostriction coefficient β measured in electric fields of

Figure 7 **a** The electrical field dependence of the electrostriction coefficient of $\text{Bi}_2\text{Fe}_4\text{O}_9/\text{BiFeO}_3$ at different temperatures. **b** The temperature dependence of the electrostriction coefficient measured in electric fields of $E = 400$ and 800 V cm^{-1} .



$E = 400$ and 800 V cm^{-1} . Upon heating above room temperature, the electrostriction coefficient changes its sign and the sample compress in an external electric field as a result of the increase in the mobility of polarons in mullite. Delocalization of electrons leads to the electronic compressibility and deformation of the sample (Fig. 6c). The difference between the $\beta(T)$ curves in fields of 400 and 800 V/cm is related to the nonlinearity of the I - V characteristic (Fig. 3).

Conclusions

The composite compound based on bismuth ferrite has a strong relationship between structural, electrical and magnetic properties.

Thus, it was shown that the electric polarization exhibits the hysteresis. At low temperatures, the dipole electric polarization is realized and, above the temperature of the magnetic phase transition in mullite, the migration polarization dominates.

The correlation between the ferroelectric polarization and hysteresis of the I - V characteristic was established. The bistable current states were found.

The ME effect was founded, which consists of a linear and quadratic contribution. The linear coefficient of ME interaction has a negative sign, similar to bismuth ferrite nanowires. In the temperature range above 240 K, the quadratic ME effect prevails. Above room temperature, a contribution from migration polarization is added, which leads to an increase in the ME interaction. The ME effect is enhanced due to the induced dipole and migration polarization of mullite grains under the action of the electric field of bismuth ferrite nanoparticles as a result of the linear ME effect.

The compression of the $\text{Bi}_2\text{Fe}_4\text{O}_9/\text{BiFeO}_3$ sample under electric field above room temperature was established. The electrostriction was explained within the electron compressibility model.

Acknowledgements

This work has been supported within the state assignment of Kirensky Institute of Physics.

Author contributions

LV. Udod performed investigation, visualization, writing—original draft. S.S. Aplesnin performed

supervision, conceptualization, methodology, writing—review and editing. M.N. Sitnikov performed investigation. M.N. Molokeev performed investigation. O.B. Romanova performed investigation, validation, visualization. F.V. Zelenov performed investigation.

Data availability

The datasets generated and analyzed during the current study are available from the corresponding author upon reasonable request.

Declarations

Conflict of interest The authors declare no conflicts of interest or competing interests.

Ethical approval Not applicable.

References

- [1] Wang J, Neaton J, Zheng H, Nagarajan V, Ogale S, Liu B, Viehland D, Vaithyanathan V, Schlom D, Waghmare U (2003) Epitaxial BiFeO_3 multiferroic thin film heterostructures. *Science* 299:1719–1722. <https://doi.org/10.1126/science.1080615>
- [2] Sarkar A, Khan GG, Chaudhuri A, Das A, Mandal K (2016) Multifunctional $\text{BiFeO}_3/\text{TiO}_2$ nano-heterostructure: photoferroelectricity, rectifying transport, and nonvolatile resistive switching property. *Appl Phys Lett* 108:033112. <https://doi.org/10.1063/1.4940118>
- [3] Hong S, Choi T, Jeon JH, Kim Y, Lee H, Joo H-Y, Hwang I, Kim J-S, Sung-Oong Kang SV, Kalinin BH, Park BH (2013) Large resistive switching in ferroelectric BiFeO_3 nano-island based switchable diodes. *Adv Mater* 25:2339–2343. <https://doi.org/10.1002/adma.201204839>
- [4] Allibe J, Fusil S, Bouzheouane K, Daumont C, Sando D, Jacquet E, Deranlot C, Bibes M, Barthélémy A (2012) Room temperature electrical manipulation of giant magnetoresistance in spin valves exchange-biased with BiFeO_3 . *Nano Lett* 12:1141–1145. <https://doi.org/10.1021/nl202537y>
- [5] Yakout SM (2021) Spintronics and innovative memory devices: a review on advances in magnetoelectric BiFeO_3 . *J Supercond Nov Magn* 34:317–338

- [6] Spaldin NA, Ramesh R (2019) Advances in magnetoelectric multiferroics. *Nat Mater* 18(3):203–212. <https://doi.org/10.1038/s41563-018-0275-2>
- [7] Wu J, Fan Z, Xiao D, Zhu J, Wang J (2016) Multiferroic bismuth ferrite-based materials for multifunctional applications: ceramic bulks, thin films and nanostructures. *Prog Mater Sci* 84:335–402. <https://doi.org/10.1016/J.PMATS CI.2016.09.001>
- [8] Ederer C, Spaldin NA (2005) Weak ferromagnetism and magnetoelectric coupling in bismuth ferrite. *Phys Rev B* 71:060401(R). <https://doi.org/10.1103/PhysRevB.71.060401>
- [9] Wang YP, Yuan GL, Chen XY, Liu J-M, Liu ZG (2006) Electrical and magnetic properties of single-phased and highly resistive ferroelectromagnet BiFeO₃ ceramic. *J Phys D* 39:2019–2023. <https://doi.org/10.1088/0022-3727/39/10/006>
- [10] Pradhan AK, Zhang K, Hunter D, Dadson JB, Loutts GB, Bhattacharya P, Katiyar R, Zhang J, Sellmer DJ, Roy UN, Cui Y, Burger A (2005) Magnetic and electrical properties of single-phase multiferroic BiFeO₃. *J Appl Phys* 97:093903. <https://doi.org/10.1063/1.1881775>
- [11] Teague JR, Gerson R, James WJ (1970) Dielectric hysteresis in single crystal BiFeO₃. *Solid State Commun* 8:1073–1074. [https://doi.org/10.1016/0038-1098\(70\)90262-0](https://doi.org/10.1016/0038-1098(70)90262-0)
- [12] Tabares-Muñoz C, Rivera JP, Bezinges A, Monnier A, Schmid H (1985) Measurement of the quadratic magnetoelectric effect on single crystalline BiFeO₃. *Jpn J Appl Phys* 24:1051–1053. <https://doi.org/10.7567/JJAPS.24S2.1051>
- [13] Neaton JB, Ederer C, Waghmare UV, Spaldin NA, Rabe KM (2005) First-principles study of spontaneous polarization in multiferroic BiFeO₃. *Phys Rev B* 71:014113. <https://doi.org/10.1103/PhysRevB.71.014113>
- [14] Carranza-Celis D, Cardona-Rodríguez A, Narváez J, Moscoso-Londono O, Muraca D, Knobel M, Ornelas-Soto N, Reiber A, Ramírez JG (2019) Control of multiferroic properties in BiFeO₃ nanoparticles. *Sci Rep* 9:3182. <https://doi.org/10.1038/s41598-019-39517-3>
- [15] Naganuma H, Inoue Y, Okamura S (2008) Dependence of ferroelectric and magnetic properties on measuring temperatures for polycrystalline BiFeO₃ films. *IEEE Trans Ultrason Ferroelec Freq Contr* 55:1046–1050. <https://doi.org/10.1109/TUFFC.2008.754>
- [16] Lebeugle D, Colson D, Forget A, Viret M, Bonville P, Marucco JF, Fusil S (2007) Room-temperature coexistence of large electric polarization and magnetic order in BiFeO₃ single crystals. *Phys Rev B* 76:024116. <https://doi.org/10.1103/PhysRevB.76.024116>
- [17] Park J-G, Le MD, Jeong J, Lee S (2014) Structure and spin dynamics of multiferroic BiFeO₃. *J Phys Condens Matter* 26:433202. <https://doi.org/10.1088/0953-8984/26/43/433202>
- [18] Kubel F, Schmid H (1990) Structure of a ferroelectric and ferroelastic monodomain crystal of the perovskite BiFeO₃. *Acta Crystallogr Sect B Struct Sci* 46:698–702. <https://doi.org/10.1107/S0108768190006887>
- [19] Sosnowska I, Zvezdin AK (1995) Origin of the long period magnetic ordering in BiFeO₃. *J Magn Magn Mater* 140–144:167–168. [https://doi.org/10.1016/0304-8853\(94\)01120-6](https://doi.org/10.1016/0304-8853(94)01120-6)
- [20] Huang F, Wang Z, Xiaomei Lu, Zhang J, Min K, Lin W, Ti R, TingTing Xu, He Ju, Yue C, Zhu J (2013) Peculiar magnetism of BiFeO₃ nanoparticles with size approaching the period of the spiral spin structure. *Sci Rep* 3:2907. <https://doi.org/10.1038/srep02907>
- [21] Suastiyanti D, Maulida YN, Wijaya M (2019) Improving magnetic properties of BiFeO₃–BaFe₁₂O₁₉ solid solution by different sintering time and temperatures of sol-gel method. *Asian J Appl Sci*. <https://doi.org/10.24203/ajas.v7i5.5926>
- [22] Hooda N, Sharma R, Hooda A, Khasa S (2023) Structural, dielectric, magnetic and magnetoelectric studies of (1–x) BaFe₁₂O₁₉–xBiFeO₃ composites. *J Magn Magn Mater* 567:170347. <https://doi.org/10.1016/j.jmmm.2022.170347>
- [23] Sahu T, Behera B (2017) Investigation on structural, dielectric and ferroelectric properties of samarium-substituted BiFeO₃–PbTiO₃ composites. *J Adv Dielect* 7:1750001. <https://doi.org/10.1142/S2010135X17500011>
- [24] Perejón A, Gil-González E, Sánchez-Jiménez PE, West AR, Pérez-Maqueda LA (2019) Electrical properties of bismuth ferrites: Bi₂Fe₄O₉ and Bi₂₅FeO₃₉. *J Eur Ceram Soc* 39:330–339. <https://doi.org/10.1016/j.jeurceramsoc.2018.09.008>
- [25] Panda A, Govindaraj R, Amarendra G (2019) Magneto dielectric coupling in Bi₂Fe₄O₉. *Phys B Condens Matter* 570:206–208. <https://doi.org/10.1016/j.physb.2019.06.045>
- [26] Singh AK, Kaushik SD, Brijesh Kumar PK, Mishra A, Venimadhav V, Siruguri SP (2008) Substantial magnetoelectric coupling near room temperature in Bi₂Fe₄O₉. *Appl Phys Lett* 92:132910. <https://doi.org/10.1063/1.2905815>
- [27] Tian ZM, Yuan SL, Wang XL, Zheng XF, Yin SY, Wang CH, Liu L (2009) Size effect on magnetic and ferroelectric properties in Bi₂Fe₄O₉ multiferroic ceramics. *J Appl Phys* 106:103912. <https://doi.org/10.1063/1.3259392>
- [28] Hajra P, Maiti RP, Chakravorty D (2012) Room temperature magnetoelectric coupling in single crystal Bi₂Fe₄O₉ nanotubes grown within an anodic aluminum oxide template. *Mater Lett* 81:138–141. <https://doi.org/10.1016/j.matlet.2012.04.123>
- [29] Dutta DP, Sudakar C, Mocherla PS, Mandal BP, Jayakumar OD, Tyagi AK (2012) Enhanced magnetic and ferroelectric properties in scandium doped nano Bi₂Fe₄O₉. *Mater*

- Chem Phys 135:998e1004. <https://doi.org/10.1016/j.matchemphys.2012.06.005>
- [30] Salami M, Mirzaee O, Honarbakshsh-Raouf A, Lavasani SANA, Moghadam AK (2017) Structural, morphological and magnetic parameters investigation of multiferroic (1-x) Bi₂Fe₄O_{9-x}CoFe₂O₄ nanocomposite ceramics. *Ceram Int* 43:4701–14709. <https://doi.org/10.1016/j.ceramint.2017.07.199>
- [31] Zvezdin AK, Pyatakov AP (2004) Phase transitions and giant magnetoelectric effect in multiferroics. *Phys Usp* 174:416–421. <https://doi.org/10.3367/UFNr.0174.200404n.0465>
- [32] Zhdanov AG, Zvezdin AK, Pyatakov AP, Oblique TB, Viehland D (2006) Effect of an electric field on magnetic transitions “incommensurate–commensurate phase” in a multiferroic of the BiFeO₃ type. *Solid St Phys* 48:83–89. <https://doi.org/10.1134/S1063783406010185>
- [33] Kadomtseva AM, Zvezdin AK, Popov YuF, Pyatakov AP, Vorobiev GP (2004) Broken parity regarding space-time inversion and magnetoelectric interaction in antiferromagnets. *Lett JETP* 79:705–716
- [34] Lee D, Kim MG, Ryu S, Jang HM, Lee SG (2005) Epitaxially grown La-modified BiFeO₃ magnetoferroelectric thin films. *Appl Phys Lett* 86:222903. <https://doi.org/10.1063/1.1941474>
- [35] Maity T, Goswami S, Bhattacharya D, Roy S (2013) Super-spin glass mediated giant spontaneous exchange bias in a nanocomposite of BiFeO₃-Bi₂Fe₄O₉. *PRL* 110:107201. <https://doi.org/10.1103/PhysRevLett.110.107201>
- [36] Maity T, Roy S (2020) Asymmetric ascending and descending loop shift exchange bias in Bi₂Fe₄O₉-BiFeO₃ nanocomposites. *J Magn Magn Mater* 494:165783. <https://doi.org/10.1016/j.jmmm.2019.165783>
- [37] Amirov AA, Batdalov AB, Kallaev SN, Omarov ZM, Verbenko IA, Razumovskaya ON, Reznichenko LA, Shilkina LA (2009) Specific features of the thermal, magnetic, and dielectric properties of multiferroics BiFeO₃ and Bi_{0.95}La_{0.05}FeO₃. *Phys Solid State* 51:1189–1192. <https://doi.org/10.1134/S1063783409060183>
- [38] Amirov AA, Kamilov IK, Batdalov AB, Verbenko IA, Razumovskaya ON, Reznichenko L, Shilkina L (2008) Magnetoelectric interactions in BiFeO₃, Bi_{0.95}Nd_{0.05}FeO₃, and Bi_{0.95}La_{0.05}FeO₃ multiferroics. *Tech Phys Lett* 34(9):760–762. <https://doi.org/10.1134/S1063785008090125>
- [39] Udod LV, Aplesnin SS, Sitnikov MN, Eremin EV, Molo-keev MS, Shabanov AV, Romanova OB, Kharkov AM (2023) Structural and magnetic transitions in the Bi₂Fe₄O₉/BiFeO₃ composite. *J Alloys Compd* 958:170445. <https://doi.org/10.1016/j.jallcom.2023.170445>
- [40] Tutov AG, Markin VN (1970) The X-ray structural analysis of the antiferromagnetic Bi₂Fe₄O₉ and the isotypical combinations Bi₂Ga₄O₉ and Bi₂A₁₄O₉. *Neorg Mater* 6:2014–2017
- [41] Moreau JM, Michel C, Gerson R, James WJ (1971) Ferroelectric BiFeO₃ X-ray and neutron diffraction study. *J Phys Chem Solids* 32:1315–1320. [https://doi.org/10.1016/S0022-3697\(71\)80189-0](https://doi.org/10.1016/S0022-3697(71)80189-0)
- [42] Bruker AXS (2008) TOPAS V4: general profile and structure analysis software for powder diffraction data. – user’s manual, Bruker AXS, Karlsr. Ger
- [43] Kirsch A, Murshed MM, Litterst FJ, Gesing TM (2019) Structural, spectroscopic, and thermoanalytic studies on Bi₂Fe₄O₉: tunable properties driven by nano- and polycrystalline states. *J Phys Chem C* 123:3161–3171. <https://doi.org/10.1021/ACS.JPCC.8B09698>
- [44] Jarrier R, Marti X, Herrero-Albillos J, Ferrer P, Haumont R, Gemeiner P, Geneste G, Berthet P, Schüllli T, Cevc P, Blinc R, Wong Stanislaus S, Tae-Jin P, Alexe M, Carpenter MA, Scott JF, Catalan G, Dkhil B (2012) Surface phase transitions in BiFeO₃ below room temperature. *Phys Rev B* 85:184104. <https://doi.org/10.1103/PhysRevB.85.184104>
- [45] Iliev MN, Litvinchuk AP, Hadjiev VG, Gospodinov MM, Skumryev V, Ressouche E (2010) Phonon and magnon scattering of antiferromagnetic Bi₂Fe₄O₉. *Phys Rev B* 81:024302. <https://doi.org/10.1103/PhysRevB.81.024302>
- [46] Aplesnin SS, Udod LV, Sitnikov MN, Velikanov DA, Molo-keev MN, Romanova OB, Shabanov AV (2022) Enhancement of ferromagnetism and ferroelectricity by oxygen vacancies in mullite Bi₂Fe₄O₉ in the Bi₂(Sn_{0.7}Fe_{0.3})₂O_{7-x} matrix. *J Magn Magn Mater* 559:169530. <https://doi.org/10.1016/j.jmmm.2022.169530>
- [47] Lebeugle D, Colson D, Forget A, Viret M (2007) Very large spontaneous electric polarization in BiFeO₃ single crystals at room temperature and its evolution under cycling fields. *Appl Phys Lett* 91:022907. <https://doi.org/10.1063/1.2753390>
- [48] Hill RM (1976) Variable-range hopping. *Phys Status Solidi A* 34:601–613. <https://doi.org/10.1002/pssa.2210340223>
- [49] Lorenz B, Wang YQ, Sun YY, Chu CW (2004) Large magnetodielectric effects in orthorhombic HoMnO₃ and YMnO₃. *Phys Rev B* 70:212412. <https://doi.org/10.1103/PhysRevB.70.212412>
- [50] Hanamura E, Hagita K, Tanabe Y (2003) Clamping of ferroelectric and antiferromagnetic order parameters of YMnO₃. *J Phys Condens Matter* 15:L103–L109. <https://doi.org/10.1088/0953-8984/15/3/102>
- [51] Ressouche E, Simonet V, Canals B, Gospodinov M, Skumryev V (2009) Magnetic frustration in an iron-based Cairo

- pentagonal lattice. *Phys Rev Lett* 103:267204. <https://doi.org/10.1103/PhysRevLett.103.267204>
- [52] Pyatakov AP, Zvezdin AK (2012) Magnetoelectric and multiferroic media. *Phys Usp* 55:557–581. <https://doi.org/10.3367/UFNe.0182.201206b.0593>
- [53] Kittel C (1960) *Elementary statistical physics*. Moscow, pp. 228–281
- [54] Sanghyun Lee MT, Fernandez-Diaz H, Kimura Y, Noda DT, Adroja SL, Junghwan Park V, Kiryukhin S-W, Cheong MM, Park J-G (2013) Negative magnetostrictive magnetoelectric coupling of BiFeO₃. *Phys Rev B* 88:060103(R). <https://doi.org/10.1103/PhysRevB.88.060103>
- [55] Moulson AJ, Herbert JM (2003) *Electroceramics: materials, properties, applications*. John Wiley & Sons

Publisher's Note Springer Nature remains neutral with regard to jurisdictional claims in published maps and institutional affiliations.

Springer Nature or its licensor (e.g. a society or other partner) holds exclusive rights to this article under a publishing agreement with the author(s) or other rightsholder(s); author self-archiving of the accepted manuscript version of this article is solely governed by the terms of such publishing agreement and applicable law.